Available online at www.sciencedirect.com
ScienceDirect
Polymer 48 (2007) 6491–6500
polymer
www.elsevier.com/locate/polymer

Homo- and *R*/*S*-copolymerizations of chiral methylpropargyl esters carrying pyrene moieties, and optical properties of the formed polymers

Jinqing Qu, Yuji Suzuki, Masashi Shiotsuki, Fumio Sanda*, Toshio Masuda*

Department of Polymer Chemistry, Graduate School of Engineering, Kyoto University, Katsura Campus, Kyoto 615-8510, Japan

Received 20 July 2007; received in revised form 5 September 2007; accepted 5 September 2007
Available online 12 September 2007

Abstract

Pyrene-functionalized chiral methylpropargyl esters, (*R*)-3-butyn-2-yl-1-pyrenebutyrate [(*R*)-**1**], (*S*)-3-butyn-2-yl-1-pyrenebutyrate [(*S*)-**1**], (*R*)-3-butyn-2-yl-1-pyrenecarboxylate [(*R*)-**2**], and 3-butyn-2-yl-1-pyrenecarboxylate [(*R*,*S*)-**2**] were polymerized with (nbd)$Rh^+[\eta^6$-$C_6H_5B^-(C_6H_5)_3]$ to obtain the corresponding polymers with moderate molecular weights (M_n: 10 500–66 500) in good yields (82–97%). All the polymers were soluble in $CHCl_3$, CH_2Cl_2, and THF. The polarimetric and CD spectroscopic data indicated that poly[(*R*)-**1**], poly[(*S*)-**1**], and poly[(*R*)-**2**] existed in a helical structure with predominantly one-handed screw sense in these solvents. The helical structure of poly[(*R*)-**1**] and poly[(*S*)-**1**] was stable upon heating and addition of MeOH, while that of poly[(*R*)-**2**] changed upon MeOH addition. The copolymerization of (*R*)-**1** with (*S*)-**1** was also conducted to obtain the copolymers satisfactorily. Poly[(*R*)-**1**], poly[(*S*)-**1**], and poly[(*R*)-**2**] emitted fluorescence smaller than the corresponding racemic copolymers. The fluorescence intensity was tuned by the addition of MeOH to THF solutions of the polymers.

Keywords: Fluorescence; Helical polyacetylene; Pyrene

1. Introduction

Pyrene and its derivatives have attracted special attention because of their valuable photophysical properties such as environmentally responsive emission of fluorescence, long-lived excited state, and excimer formation. These characteristics of pyrene and its derivatives are suitable for the application as a sensor to microscopically probe an environment around the molecules [1]. Meanwhile, considerable effort is devoted to chromophore-functionalized polymer systems, because chromophores linked to polymers show unique behavior different from free ones [2]. Secondary structures of polymers largely influence the performance of polymer-linked chromophores especially in the case of helical polymers, in which the chromophores are regularly arranged along the polymer chain. They can efficiently transport excitation energy and charge one-dimensionally along the helical polymer backbone, and thus they can be regarded as potential molecular wires, which are applicable to microprocessors and other devices [3]. For this purpose, most studies have focused on polypeptides as candidates because they can form secondary structures such as α-helix and β-sheet, where the side chains are arranged at regular intervals along the peptide main chain [4].

Substituted polyacetylenes exhibit unique properties such as semiconductivity, high gas permeability, nonlinear optical properties, and helix formation [5]. Helical polyacetylene gather interest not only from fundamental viewpoints regarding synthesis and properties, but also from practical applications, because they exhibit useful functions resulting from the regulated secondary structure, which include chiral discrimination and catalytic activity for asymmetric synthesis [6]. Incorporation of pyrene into the side chains of helical polyacetylenes enables us to develop novel functional polymers

* Corresponding authors. Tel.: +81 75 383 2589; fax: +81 75 383 2590.
E-mail addresses: sanda@adv.polym.kyoto-u.ac.jp (F. Sanda), masuda@adv.polym.kyoto-u.ac.jp (T. Masuda).

0032-3861/$ - see front matter © 2007 Elsevier Ltd. All rights reserved.
doi:10.1016/j.polymer.2007.09.012

based on synergistic actions of pyrene with conjugated helical main chain. These polymers may form helical pyrene strands as well as a helical polyacetylene main chain, leading to unique chromophore functions besides chiroptical properties. In fact, helical poly(*N*-propargylamides) carrying pyrene side chains change the conformation according to temperature, solvent [7a], and chiral–achiral composition [7b], leading to not only a change of the main chain-based absorption but also a change of fluorescence property of the side chain chromophore. The arrangement of pyrene moieties is largely affected by the helical main chain, which makes it possible to tune excimer-based fluorescence [7c]. Thus, pyrene-functionalized helical polyacetylenes are expected as stimuli-responsive photo-functional materials. A wide variety of chiral substituents have been employed as a chiral source to induce a predominantly one-handed helical structure in substituted polyacetylenes such as chiral carboxylic acids [8], alcohols [9], amino acids [10], sugars [11], terpenes [12], and so forth. We have recently found that chiral 1-methylpropargyl alcohol serves as a powerful helical source for substituted polyacetylenes [13]. Poly(1-methylpropargyl esters) easily synthesizable from this simple alcohol take a helical structure stabilized by steric repulsion between the side chains with a chiral carbon atom adjacent to the main chain. In this article, we disclose the synthesis, homo- and copolymerizations of novel optically active 1-methylpropargyl esters carrying pendent pyrene groups (Scheme 1), secondary structure of the obtained polymers, and their fluorescence property.

2. Experimental section

2.1. Measurements

^{1}H (400 MHz) and ^{13}C (100 MHz) NMR spectra were recorded on a JEOL EX-400 spectrometer using tetramethylsilane (TMS) as an internal standard. IR spectra were measured using a JASCO FT/IR-4100 spectrophotometer. Melting points (mp) were measured on a Yanaco micromelting point apparatus. Elemental analysis was conducted at the Kyoto University Elemental Analysis Center. The number- and weight-average molecular weights (M_n and M_w) of polymers were determined by gel permeation chromatography (GPC) on a JASCO Gulliver system (PU-980, CO-965, RI-930, and UV-1570) equipped with polystyrene gel columns (Shodex columns K804, K805, and J806), using tetrahydrofuran (THF) as an eluent at a flow rate of 1.0 mL/min, calibrated with polystyrene standards at 40 °C. Specific rotations ($[\alpha]_D$) were measured on a Jasco DIP-1000 digital polarimeter with a sodium lamp as a light source. CD and UV–vis spectra were recorded in a quartz cell (thickness: 1 cm) using a JASCO J-820 spectropolarimeter. Fluorescence measurements were carried out using a JASCO FP-750 spectrofluorometer.

2.2. Materials

(*R*)-(+)-3-Butyn-2-ol (Aldrich), (*S*)-(−)-3-butyn-2-ol (Aldrich), (*R*,*S*)-3-butyn-2-ol (TCI), 1-pyrenebutyric acid (Aldrich), 1-pyrenecarboxylic acid (Aldrich), *N*-(3-dimethylaminopropyl)-*N*′-ethylcarbodiimide hydrochloride (EDC·HCl; Eiweiss), and 4-dimethylaminopyridine (DMAP; Wako) were purchased and used without further purification. (nbd)Rh$^+$[η^6-$C_6H_5B^-(C_6H_5)_3$] (nbd = 2,5-norbornadiene) was prepared by the reaction of [(nbd)RhCl]$_2$ with $NaB(C_6H_5)_4$ as described in the literature [14]. Solvents used for polymerization were distilled before use according to the standard procedures.

2.3. Monomer synthesis

(*R*)-3-Butyn-2-yl-1-pyrenebutyrate [(*R*)-**1**] was synthesized as follows. 1-Pyrenebutyric acid (1.0 g, 3.5 mmol) was added to a solution of EDC·HCl (0.73 g, 3.8 mmol) and DMAP (42 mg, 0.34 mmol) in CH_2Cl_2 (45 mL) at room temperature. (*R*)-(+)-3-Butyn-2-ol (0.25 g, 3.6 mmol) was added to the solution, and the resulting mixture was stirred at room temperature overnight. The reaction mixture was washed with water (50 mL) three times, and the organic layer was dried over anhydrous $MgSO_4$. It was filtered, and the filtrate was

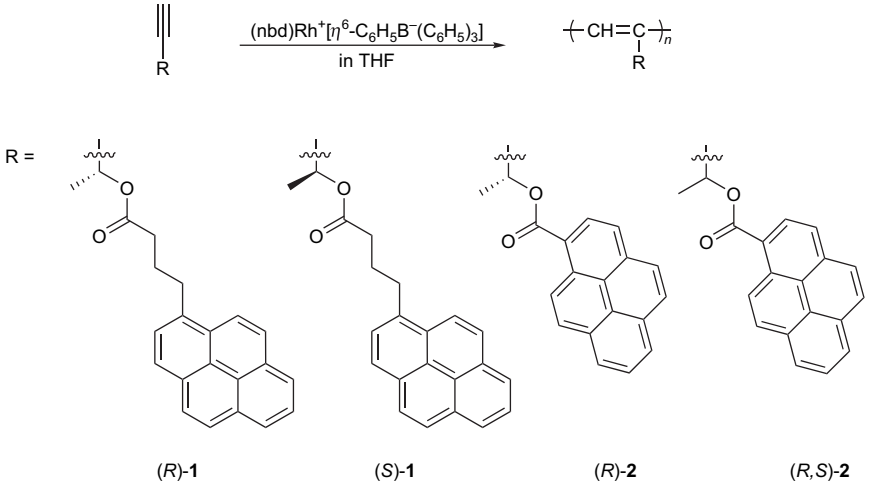

Scheme 1.

concentrated on a rotary evaporator. The residual mass was purified by silica gel column chromatography eluted with *n*-hexane/ethyl acetate = 4/1 (volume ratio) to give (*R*)-**1** as a pale yellow solid in 81% yield. Mp = 36.0–38.0 °C. $[\alpha]_D = +46.6°$ ($c = 0.10$ g/dL, in THF, room temperature). ^{1}H NMR (400 MHz, δ in ppm, $CDCl_3$): 1.51 (d, $J = 6.8$ Hz, 3H, COCH*Me*), 2.14–2.22 (m, 2H, $COCH_2CH_2$), 2.44–2.47 (m, 3H, $COCH_2$, C≡C*H*), 3.34–3.38 (m, 2H, CH_2Ar), 5.48 (q, $J = 6.8$ Hz, 1H, COC*H*Me), 7.81–7.83 (m, 1H, Ar), 7.94–7.99 (m, 4H, Ar), 8.06–8.24 (m, 3H, Ar), 8.26–8.28 (m, 1H, Ar). ^{13}C NMR (100 MHz, δ in ppm, $CDCl_3$): 21.2 ($CHCH_3$), 26.7 (CH_2CH_2COO), 32.6 (CH_2COO), 33.8 (CH_2Ar), 59.9 ($CHCH_3$), 72.9 (HC≡), 82.2 (HC≡*C*), 123.3, 124.7, 124.8, 124.9, 125.0, 125.1, 125.8, 126.7, 127.3, 127.4, 127.5 128.7, 130.0, 130.8, 131.4, 135.5, 172.2. IR (cm^{-1}, KBr): 3290 (≡C–H), 3039, 2938, 2867, 2121 (C≡C), 1735 (C=O), 1600, 1454, 1415, 1373, 1315, 1241, 1184, 1160, 1091, 1029, 845, 760, 713, 679, 528. Anal. Calcd for $C_{24}H_{20}O_2$: C, 84.68; H, 5.92. Found: C, 84.79, H, 6.22.

(*S*)-3-Butyn-2-yl-1-pyrenebutyrate [(*S*)-**1**] was synthesized from (*S*)-(−)-3-butyn-2-ol and 1-pyrenebutyric acid, and purified similarly to (*R*)-**1**. Pale yellow solid. Yield 84%. Mp = 38.0–39.0 °C. $[\alpha]_D = -46.6°$ ($c = 0.1$ g/dL in THF). ^{1}H NMR (400 MHz, δ in ppm, $CDCl_3$): 1.51 (d, $J = 6.8$ Hz, 3H, COCH*Me*), 2.16–2.20 (m, 2H, $COCH_2CH_2$), 2.42–2.46 (m, 3H, $COCH_2$, C≡C*H*), 3.34–3.38 (m, 2H, CH_2Ar), 5.48–5.49 (m, 1H, COC*H*Me), 7.80–7.82 (m, 1H, Ar), 7.94–7.99 (m, 4H, Ar), 8.05–8.14 (m, 3H, Ar), 8.25–8.28 (m, 1H, Ar). ^{13}C NMR (100 MHz, δ in ppm, $CDCl_3$): 21.2 ($CHCH_3$), 26.7 (CH_2CH_2COO), 32.6 (CH_2COO), 33.8 (CH_2Ar), 59.9 ($CHCH_3$), 72.9 (HC≡), 82.1 (HC≡*C*), 123.3, 124.7, 124.8, 124.9, 125.0, 125.1, 125.8, 126.7, 127.3, 127.4, 127.5 128.7, 130.0, 130.8, 131.4, 135.5, 172.2. IR (cm^{-1}, KBr): 3278 (≡C–H), 3039, 2985, 2935, 2117 (C≡C), 1743 (C=O), 1585, 1454, 1369, 1303, 1242, 1149, 1092, 1030, 841, 764, 656, 528. Anal. Calcd for $C_{24}H_{20}O_2$: C, 84.68; H, 5.92. Found: C, 84.30, H, 5.86.

(*R*)-3-Butyn-2-yl-1-pyrenecarboxylate [(R)-**2**] was synthesized from (*R*)-(+)-3-butyn-2-ol and 1-pyrenecarboxylic acid, and purified similarly to (*R*)-**1**. Pale yellow solid. Yield 93%. Mp = 93.0–95.0 °C. $[\alpha]_D = +36.5°$. ^{1}H NMR (400 MHz, δ in ppm, $CDCl_3$): 1.77 (d, $J = 6.6$ Hz, 3H, COCH*Me*), 2.58 (s, 1H, C≡C*H*), 5.88–5.92 (m, 1H, COC*H*Me), 7.97–8.07 (m, 5H, Ar), 8.12–8.17 (m, 2H, Ar), 8.57–8.59 (m, 1H, Ar), 9.20–9.23 (m, 1H, Ar). ^{13}C NMR (100 MHz, δ in ppm, $CDCl_3$): 21.5 ($CHCH_3$), 60.7 ($CHCH_3$), 73.2 (HC≡), 82.5 (HC≡*C*), 122.6, 124.0, 124.7, 126.2, 126.3, 127.0, 128.5, 129.5, 129.6, 130.2, 130.8, 131.3, 134.4, 166.6. IR (cm^{-1}, KBr): 3263 (≡C–H), 3043, 2985, 2935, 2117 (C≡C), 1693 (C=O), 1597, 1380, 1307, 1249, 1223, 1195, 1137, 1087, 848, 713, 663, 532. Anal. Calcd for $C_{21}H_{14}O_2$: C, 84.54; H, 4.73. Found: C, 84.67, H, 4.73.

3-Butyn-2-yl-1-pyrenecarboxylate [(*R*,*S*)-**2**] was synthesized from (*R*,*S*)-3-butyn-2-ol and 1-pyrenecarboxylic acid, and purified similarly to (*R*)-**1**. Pale yellow solid. Yield 89%. Mp = 86.5–88.0 °C. ^{1}H NMR (400 MHz, δ in ppm, $CDCl_3$): 1.77 (d, $J = 6.8$ Hz, 3H, COCH*Me*), 2.58 (s, 1H, C≡C*H*), 5.88–5.89 (m, 1H, COC*H*Me), 7.97–8.09 (m, 5H, Ar), 8.15–8.20 (m, 2H, Ar), 8.60–8.61 (m, 1H, Ar), 9.22–9.24 (m, 1H, Ar). ^{13}C NMR (100 MHz, δ in ppm, $CDCl_3$): 21.5 ($CHCH_3$), 60.7 ($CHCH_3$), 73.1 (HC≡), 82.4 (HC≡*C*), 122.7, 124.0, 124.7, 126.2, 126.3, 127.0, 128.5, 129.5, 129.6, 130.2, 130.8, 131.3, 134.4, 166.6. IR (cm^{-1}, KBr): 3278 (≡C–H), 3039, 2985, 2935, 2121 (C≡C), 1708 (C=O), 1592, 1376, 1323, 1245, 1226, 1192, 1134, 1088, 841, 706, 644, 532. Anal. Calcd for $C_{21}H_{14}O_2$: C, 84.54; H, 4.73. Found: C, 83.94, H, 4.73.

2.4. (Co)polymerization

All the polymerizations were carried out in a glass tube equipped with a three-way stopcock under nitrogen. (nbd)Rh$^+$[η^6-$C_6H_5B^-(C_6H_5)_3$] was added to a THF solution of monomers under dry nitrogen, and the resulting solution ($[M]_{0\ total}/[Rh] = 100$) was kept at 30 °C for 24 h. After that, it was poured into a large amount of MeOH to precipitate a polymer. It was separated by filtration using a membrane filter (ADVANTEC H100A047A) and dried under reduced pressure.

2.5. Spectroscopic data of the polymers

2.5.1. Poly[(*R*)-*1*]

$[\alpha]_D = -388°$ ($c = 0.10$ g/dL, in THF, room temperature). ^{1}H NMR (δ in ppm, $CDCl_3$): 1.30–1.49 (br, 3H, COCH*Me*), 1.71 (br, 2H, $COCH_2CH_2$), 2.15 (br, 2H, $COCH_2$), 2.70 (br, 2H, CH_2Ar), 5.70 (br, 1H, COC*H*Me), 6.48 (br, 1H, >C=C*H*– in the main chain of polyacetylene), 7.08–7.64 (br, 9H, Ar). IR (KBr): 3039, 2931, 2870, 1728 (C=O), 1600, 1454, 1369, 1242, 1180, 1068, 845, 756, 470 cm^{-1}.

2.5.2. Poly[(*S*)-*1*]

$[\alpha]_D = +353°$ ($c = 0.10$ g/dL, in THF, room temperature). ^{1}H NMR (δ in ppm, $CDCl_3$): 1.31–1.51 (br, 3H, COCH*Me*), 1.71 (br, 2H, $COCH_2CH_2$), 2.13 (br, 2H, $COCH_2$), 2.70 (br, 2H, CH_2Ar), 5.71 (br, 1H, COC*H*Me), 6.47 (br, 1H, >C=C*H*– in the main chain of polyacetylene), 7.08–7.64 (br, 9H, Ar). IR (KBr): 3039, 2935, 2870, 1732 (C=O), 1600, 1454, 1369, 1254, 1184, 1072, 845, 756, 485 cm^{-1}.

2.5.3. Poly[(*R*)-*2*]

$[\alpha]_D = -244°$ ($c = 0.10$ g/dL, in THF, room temperature). ^{1}H NMR (δ in ppm, $CDCl_3$): 1.59 (br, 3H, COCH*Me*), 5.80 (br, 1H, COC*H*Me), 6.43 (br, 1H, >C=C*H*– in the main chain of polyacetylene), 7.25–8.00 (br, 7H, Ar), 8.58 (br, 1H, Ar), 9.03 (br, 1H, Ar). IR (KBr): 3039, 2973, 2931, 1704 (C=O), 1592, 1446, 1376, 1254, 1195, 1084, 894, 844, 752, 705, 462 cm^{-1}.

2.5.4. Poly[(*R*,*S*)-*2*]

^{1}H NMR (δ in ppm, $CDCl_3$): 1.55 (br, 3H, COCH*Me*), 5.70 (br, 1H, COC*H*Me), 6.44 (br, 1H, >C=C*H*– in the main chain of polyacetylene), 7.25–8.00 (br, 7H, Ar), 8.59 (br, 1H, Ar), 9.05 (br, 1H, Ar). IR (KBr): 3039, 2973, 2931, 1704

(C=O), 1627, 1592, 1542, 1504, 1446, 1376, 1254, 1195, 1133, 1084, 1038, 894, 844, 752, 705, 462 cm^{-1}.

2.5.5. Poly[(R)-**1**$_{50}$-co-(S)-**1**$_{50}$)]

^{1}H NMR (δ in ppm, $CDCl_3$): 1.31–1.51 (br, 3H, COCH*Me*), 1.70 (br, 2H, $COCH_2CH_2$), 2.14 (br, 2H, $COCH_2$), 2.70 (br, 2H, CH_2Ar), 5.70 (br, 1H, COC*H*Me), 6.47 (br, 1H, >C=C*H*– in the main chain of polyacetylene), 6.88–7.64 (br, 9H, Ar). IR (KBr): 3039, 2931, 2869, 1727 (C=O), 1600, 1454, 1369, 1241, 1180, 1068, 841, 756, 482 cm^{-1}.

3. Results and discussion

3.1. Monomer synthesis

Monomers (*R*)-**1**, (*S*)-**1**, (*R*)-**2**, and (*R*,*S*)-**2** were synthesized by the reaction of 1-pyrenebutyric and 1-pyrenecarboxylic acids with the corresponding (*R*)-, (*S*)-, and (*R*,*S*)-3-butyn-2-ols using EDC·HCl and DMAP as condensation agents. The structures of the monomers were confirmed by IR, ^{1}H, and ^{13}C NMR spectroscopies besides elemental analysis.

3.2. Polymerization

Table 1 summarizes the results of the homo- and copolymerizations of (*R*)-**1** and (*S*)-**1** catalyzed by $Rh^+(nbd)[\eta^6$-$C_6H_5B^-(C_6H_5)_3]$ (1 mol%) with a total initial monomer concentration of 0.20 M in THF at 30 °C for 24 h. The enantiomerically isomeric monomers satisfactorily underwent homo- and copolymerizations to afford the corresponding polymers with M_ns in the range from 34 600 to 66 500 in 88–97% yields, which were soluble in THF, CH_2Cl_2, and $CHCl_3$, but insoluble in *n*-hexane, diethyl ether, and MeOH. The homopolymers of (*R*)-**1** and (*S*)-**1** were pale yellow, while the copolymers gradually became pale white with increase of the comonomer ratio. All the polymers displayed a unimodal GPC chromatogram, indicating that the polymerization proceeded through a single propagating species. It is likely that the unit ratios in the copolymers were almost the same as the monomer feed mole ratios judging from the high copolymer yields.

Pale white polymers were obtained in 85 and 82% yields by the polymerization of (*R*)-**2** and (*R*,*S*)-**2** as summarized in Table 2. The M_ns of the polymers (10 500 and 10 600) were lower than those of the homo- and copolymers of (*R*)-**1** and (*S*)-**1**. The solubility of poly[(*R*)-**2**] and poly[(*R*,*S*)-**2**] was the same as that of poly[(*R*)-**1**] and poly[(*S*)-**1**]. Interestingly, when the homopolymerizations of (*R*)-**2** and (*R*,*S*)-**2** were carried out with $[M]_0 = 0.20$ M, the formed polymers were insoluble in organic solvents.

Table 1
(Co)polymerization of (*R*)-**1** and (*S*)-**1**[a]

Run	Monomer feed molar ratio (*R*)-**1**/(*S*)-**1**	Yield[b] (%)	M_n[c]	M_w/M_n[c]	$[\alpha]_D$[d] (deg)
1	100/0	93	66 500	4.38	−388
2	90/10	89	61 300	4.37	−260
3	70/30	88	63 900	4.21	−152
4	50/50	95	60 900	4.45	−22
5	30/70	97	54 000	4.30	+102
6	10/90	89	46 800	3.56	+190
7	0/100	91	34 600	3.23	+353

[a] Conditions: catalyst (nbd)$Rh^+[\eta^6$-$C_6H_5B^-(C_6H_5)_3]$, $[M]_0 = 0.20$ M in THF, $[M]_0/[Rh] = 100$, 30 °C, 24 h.
[b] MeOH-insoluble part.
[c] Determined by GPC in THF on basis of polystyrene calibration.
[d] Measured by polarimetry in THF ($c = 0.100$ g/dL) at room temperature.

3.3. Polymer structure

The polymer structures were examined by IR and ^{1}H NMR spectroscopies. The monomers exhibited IR absorption bands around 3280 and 2121 cm^{-1} associated with the ≡C–H and –C≡C– stretching vibrations, while the polymers did not exhibit these peaks. The polymers display no ^{1}H NMR signal around 2.45 ppm assignable to an acetylenic proton, as shown in Fig. 1. All these results clearly indicate that acetylene polymerization took place to form polymers composed of alternating single and double bonds. The *cis* content of the main chain was quantitative, which was determined by the integration ratio between the *cis* vinyl proton and the other proton signals.

3.4. Chiroptical properties of the polymers

The secondary structures of the polymers were examined by polarimetry, CD, and UV–vis spectroscopies. The $[\alpha]_D$ values of poly[(*R*)-**1**], poly[(*S*)-**1**], and poly[(*R*)-**2**] were −388, +353, and −244° measured in THF at room temperature ($c = 0.100$ g/dL), respectively. In contrast to the corresponding monomers (+45.6, −45.6, and +35.5°), the polymers displayed large optical rotations, suggesting that they took a helical structure with predominantly one-handed screw sense. We also measured the $[\alpha]_D$ of poly[(*R*)-**1**] and poly[(*S*)-**1**] in CH_2Cl_2, $CHCl_3$, and toluene to find that the $[\alpha]_D$ was almost the same irrespective of solvents.

The top part of Fig. 2 shows the CD and UV–vis spectra of poly[(*R*)-**1**], poly[(*S*)-**1**], and poly[(*R*)-**2**] measured in THF. Poly[(*R*)-**1**] and poly[(*S*)-**1**] showed strong minus and plus CD signals at 330 nm assignable to the helical polyacetylene backbone. It was confirmed that poly[(*R*)-**1**] and poly[(*S*)-**1**] adopted predominantly one-handed helical conformations with an opposite preferred screw sense to each other.

Table 2
Polymerization of (*R*)-**2** and (*R*,*S*)-**2**[a]

Run	Monomer	Yield[b] (%)	M_n[c]	M_w/M_n[c]	$[\alpha]_D$[d] (deg)
1	(*R*)-**2**	85	10 500	2.05	−244
2	(*R*,*S*)-**2**	82	10 600	2.00	−25

[a] Conditions: catalyst (nbd)$Rh^+[\eta^6$-$C_6H_5B^-(C_6H_5)_3]$, $[M]_0 = 0.10$ M in THF, $[M]_0/[Rh] = 100$, 30 °C, 24 h.
[b] MeOH-insoluble part.
[c] Determined by GPC in THF on basis of polystyrene calibration.
[d] Measured by polarimetry in THF ($c = 0.100$ g/dL) at room temperature.

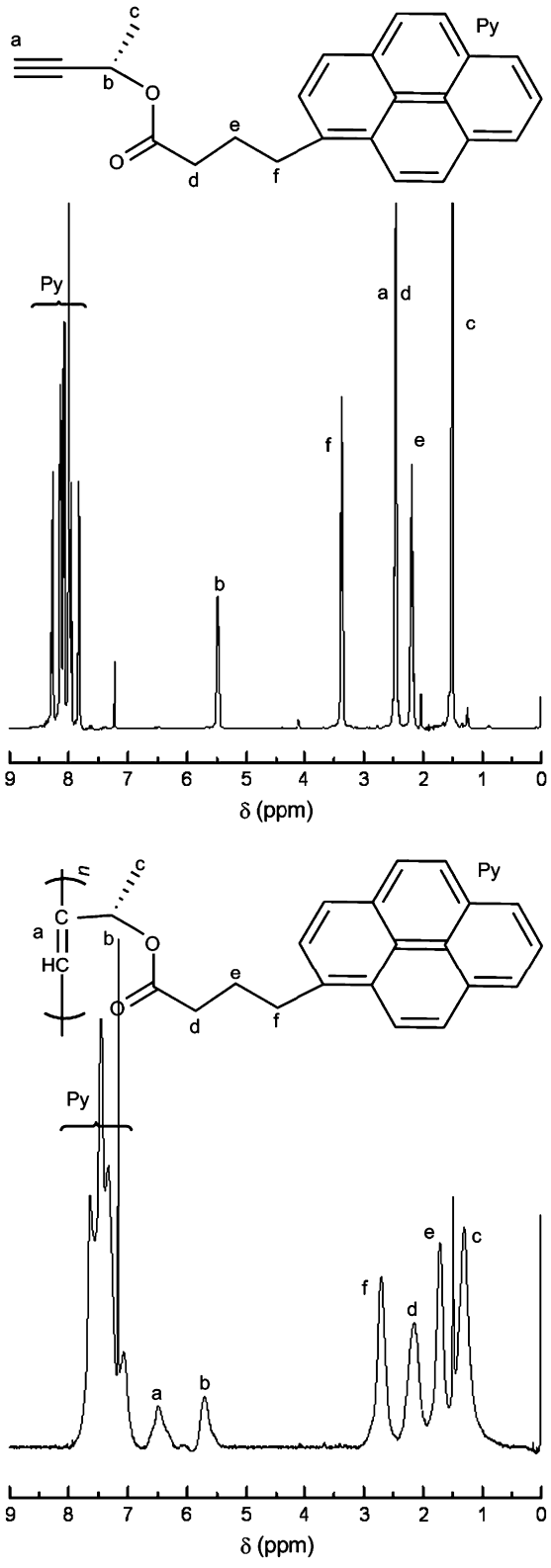

Fig. 1. ^{1}H NMR spectra (400 MHz, $CDCl_3$) of (*R*)-**1** and poly[(*R*)-**1**].

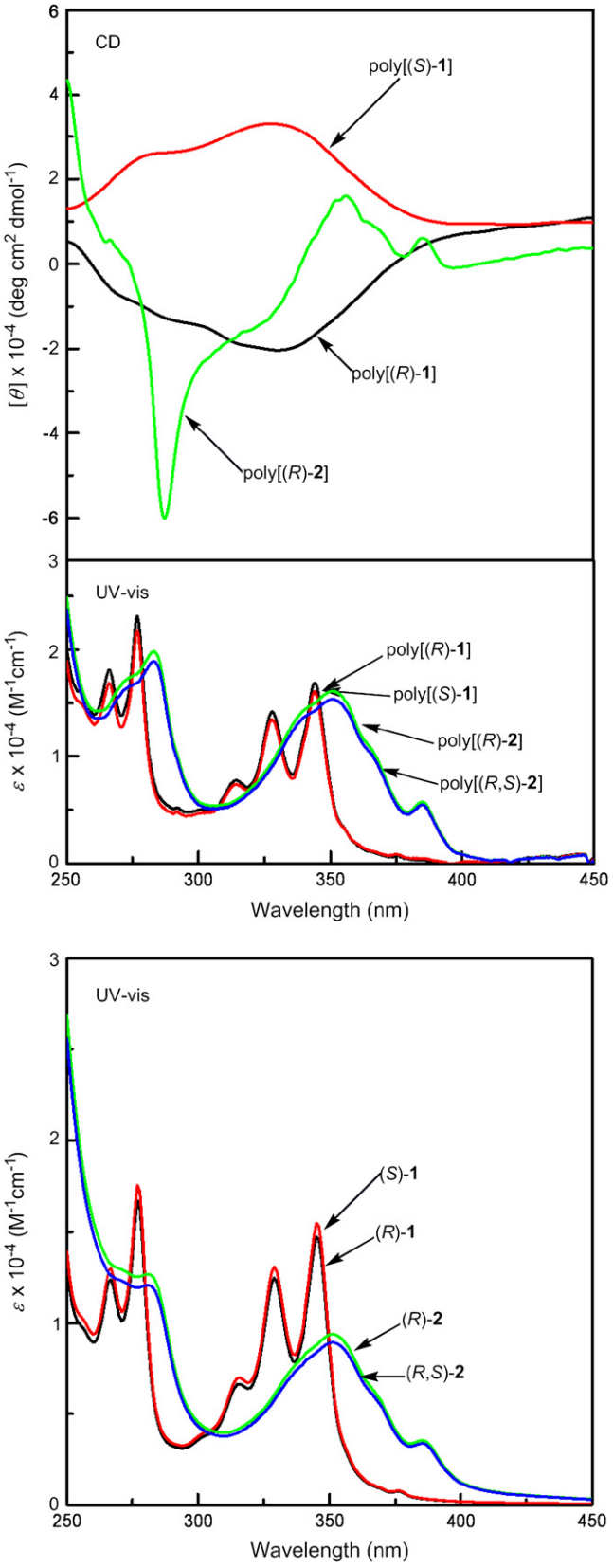

Fig. 2. CD and UV–vis spectra of poly[(*R*)-**1**], poly[(*S*)-**1**], poly[(*R*)-**2**], and poly[(*R*,*S*)-**2**] (top), and UV–vis spectra of (*R*)-**1**, (*S*)-**1**, (*R*)-**2**, and (*R*,*S*)-**2** (bottom) measured in THF at 22 °C. (*R*)-**1**, (*S*)-**1**, poly[(*R*)-**1**], and poly[(*S*)-**1**]: $c = 2.93 \times 10^{-5}$ M, (*R*)-**2** and poly[(*R*)-**2**]: $c = 3.35 \times 10^{-5}$ M.

Poly[(*R*)-**2**] possessed strong minus and plus CD signals at 285 and 365 nm, proving that it also adopted a helical conformation with preferred screw sense. Poly[(*R*)-**1**] and poly[(*S*)-**1**] exhibited UV–vis absorption peaks at 270, 280, 315, 325,

and 345 nm attributable to pyrene, which were the same positions as those of the monomers. On the other hand, poly[(*R*)-**2**] and (*R*)-**2** exhibited absorption peaks at 285, 365 and 380 nm. Judging from the wavelength and broadness, it is likely that the CD signals of poly[(*R*)-**2**] at 285, 365 and 380 nm originate from helically arrayed pyrene moieties.

Fig. 3 depicts the temperature dependence of CD and UV–vis spectra of poly[(*S*)-**1**] and poly[(*R*)-**2**] measured in THF. The intensities of Cotton effect and UV–vis absorption were almost the same irrespective of temperature at a range from −10 to 50 °C. We also measured the CD and UV–vis spectra of the polymer up to 100 °C in toluene to find slight changes (not shown). The helical structure of the polymer was thermally very stable in this temperature range. The tolerance of the helicity of the present polymer to heat is remarkably high among helical polyacetylenes, which commonly transform into random coil at this high temperature [12].

When helical structures of polyacetylenes are stabilized by the support of intramolecular hydrogen bonding like poly(*N*-propargylamides) [10], they transform into random coil by the addition of polar solvents such as MeOH due to collapse of regulated hydrogen bonding strands. Poly[(*R*)-**1**] displayed almost the same CD spectroscopic pattern irrespective of THF/MeOH composition as solvent (Fig. 4). The helical structure was very stable against polar solvents. It is noteworthy that the presence of a chiral group in a close proximity to the main chain is quite effective to induce a helix stabilized by steric repulsion between the side chains. Upon raising MeOH content, the magnitude of CD signal of poly[(*R*)-**2**] at 285 nm decreased more largely than those at 350–400 nm. Aggregation possibly took place to affect the CD spectroscopic pattern in this case, but a concrete reason is unclear.

Fig. 5 depicts the $[\alpha]_D$ of copolymers of (*R*)-**1** and (*S*)-**1** with respect to the enantiomeric excess (ee) of the monomer unit. The copolymers with a large ee showed a large $[\alpha]_D$ and an intense Cotton effect in THF, indicating that they took a helical conformation with predominantly one-handed screw sense. On the other hand, the copolymers with a small ee showed a small specific rotation and a CD signal. In the copolymerization of a pair of enantiomeric monomers, a small excess of one unit induces one-handed helicity in some cases, this is called "the majority rule" [15]. In the present (*R*)-/(*S*)-copolymerization, the majority rule was not clearly observed. The minus CD signal of poly[(*R*)-**1**] at 330 nm gradually turned into plus one (the figure is not shown) with increase of (*S*)-unit. Poly[(*R*)-$\mathbf{1}_{50}$-*co*-(*S*)-$\mathbf{1}_{50}$] exhibited almost no CD signal. The UV–vis spectral patterns of the copolymers were almost the same as those of poly[(*R*)-**1**] and poly[(*S*)-

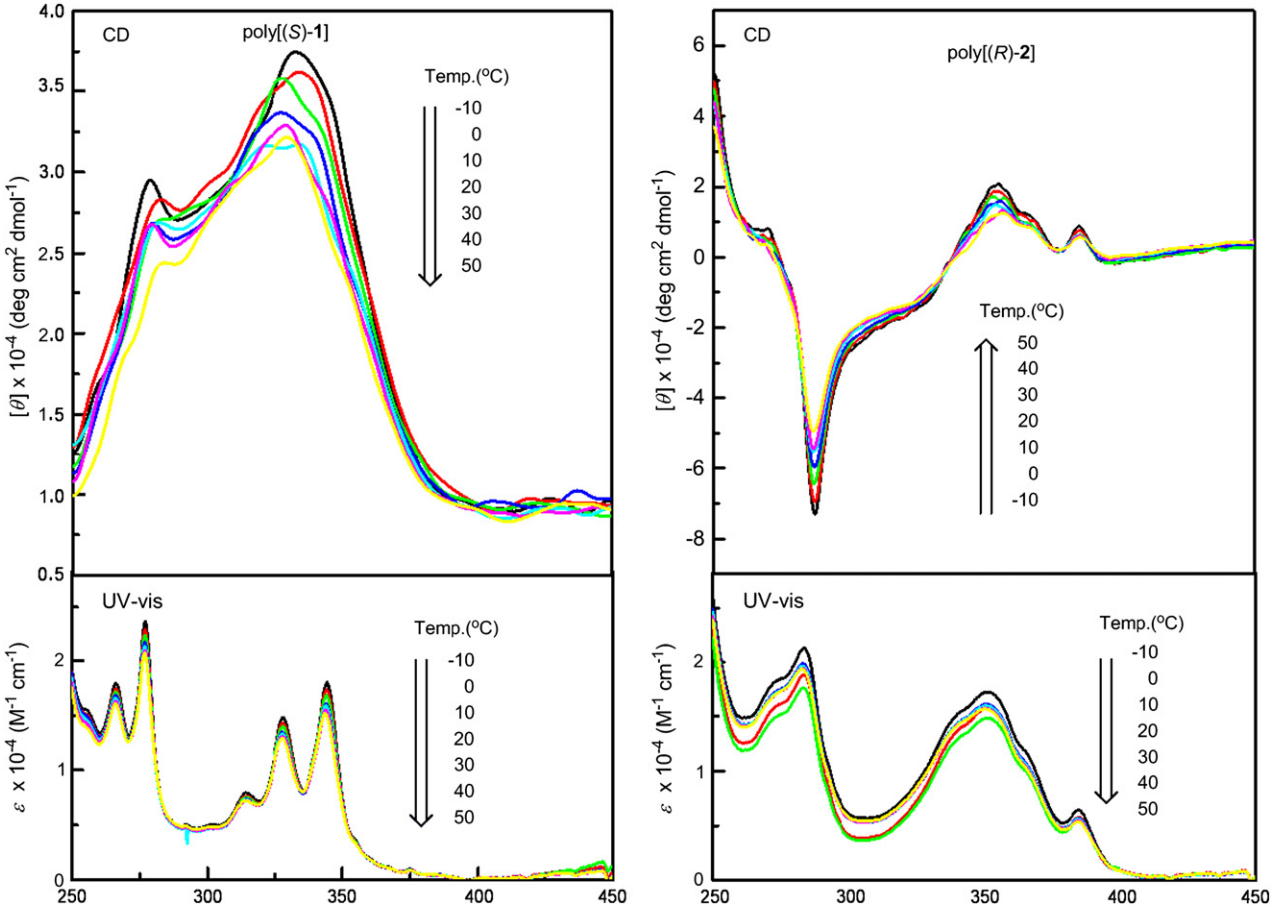

Fig. 3. CD and UV–vis spectra of poly[(*S*)-**1**] and poly[(*R*)-**2**] measured in THF at a range from −10 to 50 °C. Poly[(*S*)-**1**]: $c = 2.93 \times 10^{-5}$ M, poly[(*R*)-**2**]: $c = 3.35 \times 10^{-5}$ M].

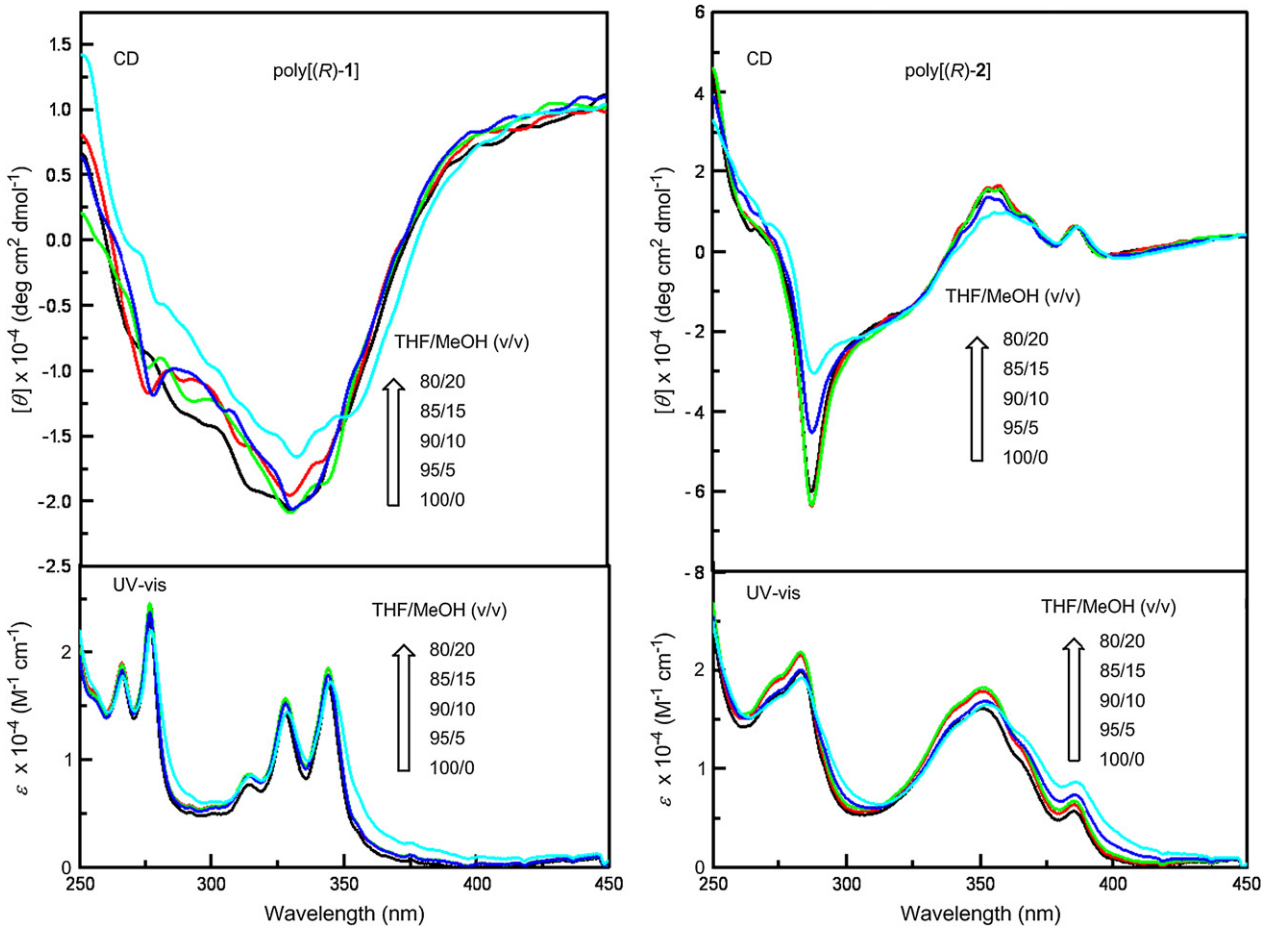

Fig. 4. CD and UV–vis spectra of poly[(*R*)-**1**] and poly[(*R*)-**2**] measured in THF/MeOH with various compositions (100/0–60/40, v/v) at 22 °C. Poly[(*R*)-**1**]: $c = 2.93 \times 10^{-5}$ M, poly[(*R*)-**2**]: $c = 3.35 \times 10^{-5}$ M.

1]. We also confirmed that the helical structure of copolymers was very stable to temperature and addition of MeOH.

3.5. Fluorescence properties of the polymers

Fig. 6 depicts the fluorescence spectra of the monomers and polymers, and Table 3 summarizes the fluorescence quantum yields (ϕ) measured in THF at room temperature. Monomers (*R*)-**1** and (*S*)-**1** emitted fluorescence at 380 and 395 nm upon excitation at 345 nm. Poly[(*R*)-**1**] and poly[(*S*)-**1**] emitted fluorescence at 385, 410, and 480 nm. The former two bands are assignable to isolated pyrene units, and the latter one is assignable to the excimer. The ϕs of poly[(*R*)-**1**] and poly[(*S*)-**1**] were almost the same (35.5 and 36.8%) regardless of helical sense, and larger than those of (*R*)-**1** and (*S*)-**1** (30.2%). On the other hand, poly[(*R*)-**2**] and poly[(*R*,*S*)-**2**] emitted excimer-based fluorescene around 520 nm upon excitation at 365 nm, whose ϕs were smaller than those of the corresponding monomers [ϕ of (*R*)-**2** and (*R*,*S*)-**2**: 95.4%). This difference may be associated with the difference in flexibility of the side chains between the polymers. The polyacetylene backbone commonly functions as a quenching site for light emission to absorb light emitted from appendages with energy

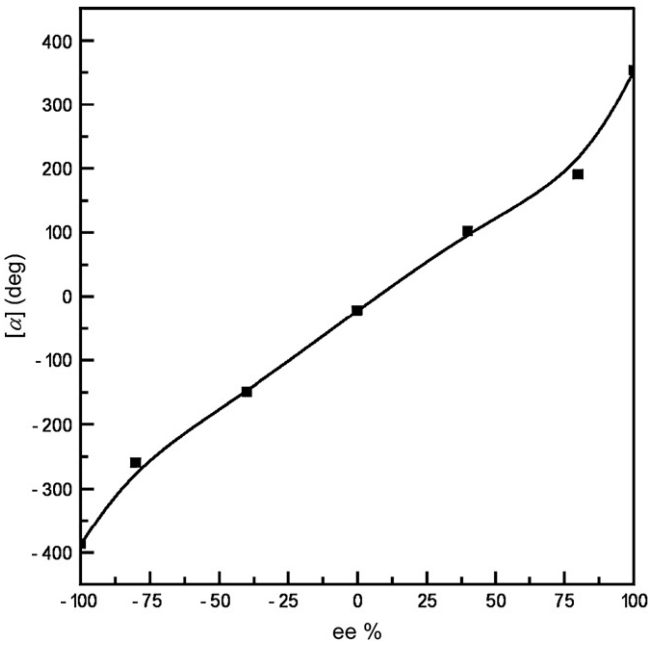

Fig. 5. Relationship between the enantiomeric excess of (*R*)-**1** unit over (*S*)-**1** unit in poly[(*R*)-**1**-*co*-(*S*)-**1**] and the $[\alpha]_D$ of the copolymer measured by polarimetry at room temperature in THF ($c = 0.100$ g/dL).

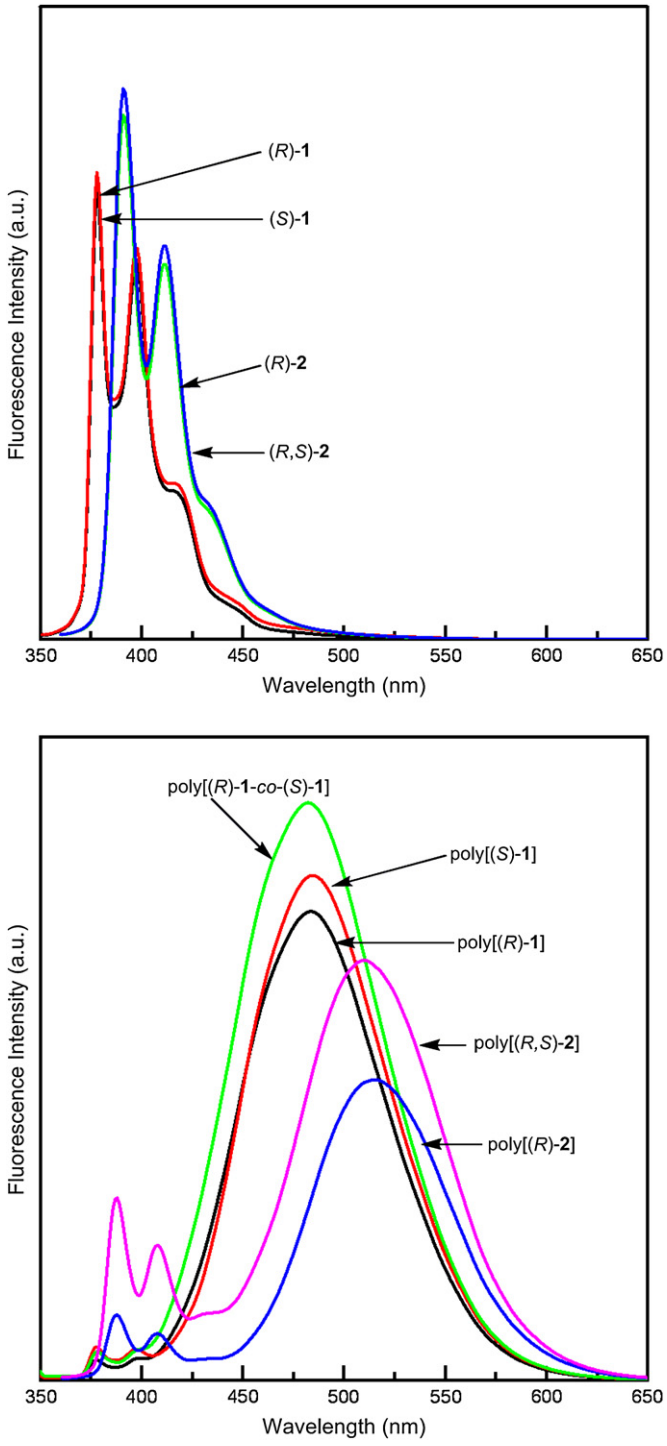

Fig. 6. Fluorescence spectra of (*R*)-**1**, (*S*)-**1**, (*R*,*S*)-**2**, poly[(*R*)-**1**], poly[(*S*)-**1**], and poly[(*R*,*S*)-**2**] measured in THF at 22 °C. The intensities are normalized based on the concentration of pyrene unit. (*R*)-**1**, (*S*)-**1**, poly[(*R*)-**1**], and poly-[(*S*)-**1**]: $c = 2.93 \times 10^{-6}$ M, excited at 345 nm. (*R*,*S*)-**2** and poly[(*R*)-**2**]: $c = 3.35 \times 10^{-6}$ M, excited at 365 nm.

dissipated via nonradiative decay, thus resulting in low photoluminescence efficiency. The pyrene moieties of poly[(*R*)-**1**] and poly[(*S*)-**1**] are more flexible than those of poly[(*R*)-**2**], because the formers are located farther from the polyacetylene main chain than those of the latters. Consequently, the polyacetylene backbone of poly[(*R*)-**1**] and poly[(*S*)-**1**] quenches

Table 3
Fluorescence quantum yields (ϕ) of the monomers and polymers[a]

Compound	Excited wavelength (nm)	ϕ (%)
(*R*)-**1**	345	30.2
(*S*)-**1**	345	30.2
Poly[(*R*)-**1**]	345	35.5
Poly[(*S*)-**1**]	345	36.8
Poly[(*R*)-$\mathbf{1}_{50}$-*co*-(*S*)-$\mathbf{1}_{50}$]	345	55.8
(*R*)-**2**	365	95.4
(*R*,*S*)-**2**	365	95.4
Poly[(*R*)-**2**]	365	57.6
Poly[(*R*,*S*)-**2**]	365	67.4

[a] Concentration: (*R*)-**1**, poly[(*R*)-**1**], poly[(*R*)-$\mathbf{1}_{50}$-*co*-(*S*)-$\mathbf{1}_{50}$]: 2.94×10^{-6} M; (*R*)-**2**, poly[(*R*)-**2**], poly[(*R*,*S*)-**2**]: 3.35×10^{-6} M.

light emission less than that of poly[(*R*)-**2**]. Under irradiation of UV-light, the monomers and polymers emitted blue and blue-green fluorescences, respectively, which were observed with naked eyes.

Fig. 7 illustrates the dependence of ϕ of the copolymer on ee measured in THF at room temperature. Upon increasing the content of (*S*)-**1** unit in the copolymer, the ϕ increased to reach the maximum (55.8%) at 0% ee. Further increase of ee led to decrease of ϕ. The ϕ of poly[(*R*)-$\mathbf{1}_{50}$-*co*-(*S*)-$\mathbf{2}_{50}$] was almost twice as large as that of poly[(*R*)-**1**] and poly-[(*S*)-**1**]. It was confirmed that the variation of polymer composition not only resulted in the difference of the secondary structure but also the fluorescence property. The pendent pyrene groups of poly[(*R*)-$\mathbf{1}_{50}$-*co*-(*S*)-$\mathbf{2}_{50}$] seem to take positions that are more favorable to form excimer than those of the homopolymers. The predominantly one-handed helical conformations of the homopolymers presumably prevent pendent pyrene groups from overlapping each other due to the rigid structure [16], leading to a low population of excimers and

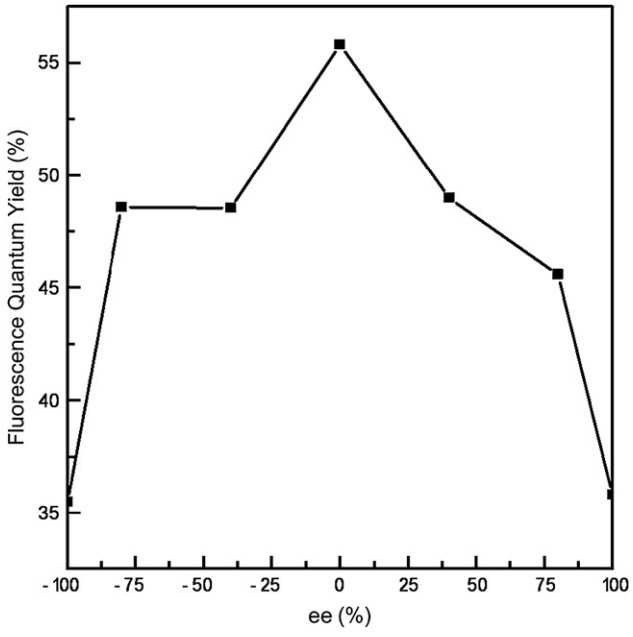

Fig. 7. Dependence of fluorescence quantum yield measured in THF at 22 °C excited at 345 nm on the enantiomeric excess of (*R*)-**1** unit over (*S*)-**1** unit in poly[(*R*)-**1**-*co*-(*S*)-**1**] ($c = 2.93 \times 10^{-6}$ M).

weak excimer-based fluorescence. Poly[(*R*)-**2**] and poly[(*R*,*S*)-**2**] exhibited a tendency regarding the fluorescence quantum yields similar to poly[(*R*)-**1**] and poly[(*R*)-$\mathbf{1}_{50}$-*co*-(*S*)-$\mathbf{1}_{50}$] as listed in Table 3.

Fig. 8 depicts the fluorescence spectra of poly[(*R*)-**1**] and poly[(*R*,*S*)-**2**] measured in THF/MeOH with various compositions. The intensity of fluorescence of poly[(*R*)-**1**] and poly[(*R*,*S*)-**2**] around 500 nm tended to decrease upon raising MeOH content. The degree of fluorescence decrease was larger than that of the CD intensity depicted in Fig. 4. It is suggested that the pyrene moieties of the side chains changed the conformation upon polarity increase of solvent, while the polyacetylene backbone did not so much.

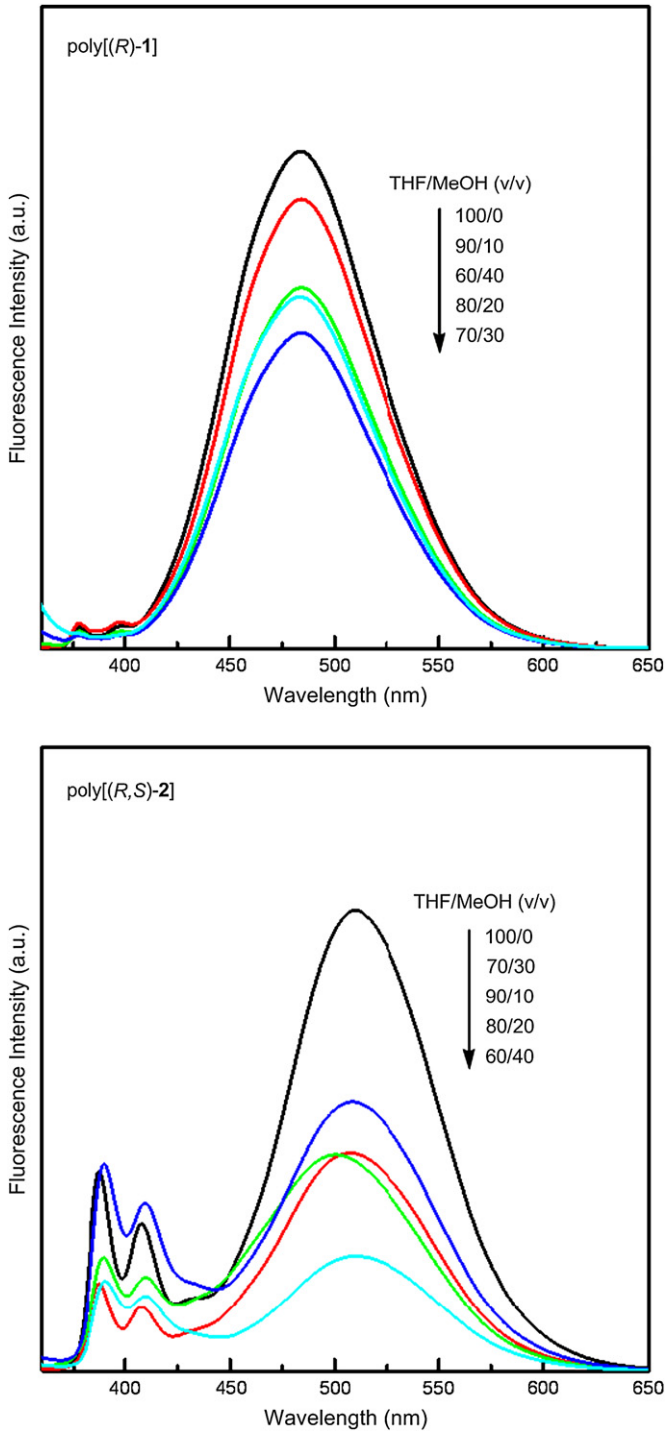

Fig. 8. Fluorescence spectral changes of poly[(*R*)-**1**] and poly[(*R*,*S*)-**2**] measured in THF/MeOH with various compositions (100/0–60/40, v/v) at 22 °C. Poly[(*R*)-**1**]: $c = 2.93 \times 10^{-6}$ M, excited at 345 nm. Poly[(*R*,*S*)-**2**]: $c = 3.35 \times 10^{-6}$ M, excited at 365 nm.

4. Conclusions

We have demonstrated the synthesis and Rh-catalyzed polymerization of novel pyrene-functionalized chiral methylpropargyl esters, (*R*)-**1**, (*S*)-**1**, (*R*)-**2**, and (*R*,*S*)-**2** to obtain the corresponding polymers with moderate molecular weights (M_n: 10 500–66 500) in good yields (82–93%). Poly[(*R*)-**1**], poly[(*S*)-**1**], and poly[(*R*)-**2**] existed in a helical structure with predominantly one-handed screw sense in THF, CH_2Cl_2, $CHCl_3$, and toluene. The helical structure of poly[(*R*)-**1**] and poly[(*S*)-**1**] was stable upon heating and addition of MeOH. The copolymerization of (*R*)-**1** with (*S*)-**1** was conducted to obtain the copolymers. The controllable secondary structure of the copolymers by various compositions led to a controlled orientation of pyrene at the side chains. The intensity of fluorescence assignable to pyrene-based excimer was tuned by the addition of MeOH to THF solutions of the polymers.

Acknowledgments

This research was partly supported by a Grant-in-Aid for Science Research in a Priority Area "Super-Hierarchical Structures (no. 446)" from the Ministry of Education, Culture, Sports, Science and Technology, Japan. Jinqing Qu acknowledges the financial support from the Ministry of Education, Culture, Sports, Science, and Technology (Monbukagakusho), Japan.

References

[1] (a) Bernhardt S, Kastler M, Enkelmann V, Baumgarten M, Klaus M. Chem Eur J 2006;12:6117–28;
(b) Ara AM, Iimori T, Yoshizawa T, Nakabayashi T, Ohta N. J Phys Chem B 2006;110:23669–77;
(c) Mitchell A, Bystryak WSM, Liu Z, Siddiqui J. Macromolecules 1998;31:6855–64.
[2] (a) Webber SE. Chem Rev 1990;90:1469–82;
(b) Guillet E. Polymer photochemistry and photophysics. Cambridge, UK: Cambridge University Press; 1985.
[3] (a) Shoji O, Higashi Y, Hishinuma S, Sato M, Annaka M, Yoshikuni M, et al. Macromolecules 2002;35:2116–21;
(b) Shoji O, Okumura M, Kuwata H, Sumida T, Kato R, Annaka M, et al. Macromolecules 2001;34:4270–6;
(c) Sato M, Yoshimoto M, Nakahira T, Iwabuchi S. Makromol Chem Rapid Commun 1993;14:179–84;
(d) Sisido M, Egusa S, Imanishi Y. J Am Chem Soc 1983;105:1041–9;
(e) Ueno A, Toda F, Iwakura Y. Biopolymers 1974;13:1213–22.
[4] Reviews: (a) Hill DJ, Mio MJ, Prince RB, Hughes TS, Moore JS. Chem Rev 2001;101:3893–4012;
(b) Sanda F, Endo T. Macromol Chem Phys 1999;200:2651–61.

[5] (a) Masuda T. J Polym Sci Part A Polym Chem 2007;45:165–80;
(b) Masuda T, Sanda F, Shiotsuki M. In: Crabtree RH, Mingos DMP, editors. Comprehensive organometallic chemistry III. Oxford: Elsevier; 2007 [chapter 11.16];
(c) Masuda T, Sanda F. In: Grubbs RH, editor. Handbook of metathesis, vol. 3. Weinheim: Wiley-VCH; 2003 [chapter 3.11].
[6] (a) Nakano T, Okamoto Y. Chem Rev 2001;101:4013–38;
(b) Okamoto Y, Nakano T. Chem Rev 1994;94:349–72.
[7] (a) Zhao H, Sanda F, Masuda T. Polymer 2006;47:1584–9;
(b) Zhao H, Sanda F, Masuda T. Macromolecules 2004;37:8893–6;
(c) Nomura R, Yamada K, Masuda T. Chem Commun 2002;478–9.
[8] (a) Tabei J, Shiotsuki M, Sanda F, Masuda T. Macromolecules 2005;38:5860–7;
(b) Tabei J, Nomura R, Shiotsuki M, Sanda F, Masuda T. Macromol Chem Phys 2005;206:323–32;
(c) Tabei J, Nomura R, Masuda T. Macromolecules 2002;35:5405–9;
(d) Nomura R, Tabei J, Masuda T. J Am Chem Soc 2001;123:8430–1.
[9] (a) Nakako H, Nomura R, Masuda T. Macromolecules 2001;34:1496–502;
(b) Nakako H, Mayahara Y, Nomura R, Tabata M, Masuda T. Macromolecules 2000;33:3978–82;
(c) Nomura R, Fukushima H, Nakako H, Masuda T. J Am Chem Soc 2000;122:8830–6;
(d) Nakako H, Nomura R, Tabata M, Masuda T. Macromolecules 1999;32:2861–4.
[10] (a) Zhao H, Sanda F, Masuda T. Polymer 2005;46:2841–6;
(b) Sanda F, Terada K, Masuda T. Macromolecules 2005;38:8149–54;
(c) Lam JWY, Tang BZ. Acc Chem Res 2005;38:745–54;
(d) Gao G, Sanda F, Masuda T. Macromolecules 2003;36:3932–7;
(e) Li BS, Cheuk KKL, Ling LS, Chen JW, Xiao XD, Bai CL, et al. Macromolecules 2003;36:77–85.
[11] (a) Kadokawa J, Tawa K, Suenaga M, Kaneko Y, Tabata MJ. Macromol Sci Part A Pure Appl Chem 2006;43:1179–87;
(b) Otsuka I, Sakai R, Satoh T, Kakuchi R, Kaga H, Kakuchi T. J Polym Sci Part A Polym Chem 2005;43:5855–63;
(c) Matuura K, Furuno S, Kobayashi K. Chem Lett 1998;847–8.
[12] Aoki T, Shinohara KI, Kaneko T, Oikawa E. Macromolecules 1996;29:4192–8.
[13] Suzuki Y, Shiotsuki M, Sanda F, Masuda T. Macromolecules 2007;40:1864–7.
[14] Schrock RR, Osborn JA. Inorg Chem 1970;9:2339–43.
[15] (a) Green MM, Peterson NC, Sato T, Teramoto A, Cook R, Lifson S. Science 1995;268:1860–5;
(b) Green MM, Park JW, Sato T, Teramoto A, Lifson S, Selinger RLB, et al. Angew Chem Int Ed 1999;38:3138–54.
[16] (a) Watkins DM, Fox MA. J Am Chem Soc 1996;118:4344–53;
(b) Fox HH, Fox MA. Macromolecules 1995;28:4570–6;
(c) Watkins DM, Fox MA. J Am Chem Soc 1994;116:6441–2.